

## Light-Addressable Potentiometric Sensor for Biochemical Systems

DEAN G. HAFEMAN, J. WALLACE PARCE, HARDEN M. MCCONNELL

Numerous biochemical reactions can be measured potentiometrically through changes in *pH*, redox potential, or transmembrane potential. An alternating photocurrent through an electrolyte-insulator-semiconductor interface provides a highly sensitive means to measure such potential changes. A spatially selectable photoresponse permits the determination of a multiplicity of chemical events with a single semiconductor device.

POTENTIOMETRIC MEASUREMENTS are commonly used in biophysical and biochemical studies. Examples include *pH* measurements with glass electrodes and redox measurements with metal electrodes. Such potentiometric measurements usually involve high input impedance measuring devices so as not to disturb the chemical equilibrium. High-impedance measurements are also used in determinations of transmembrane potentials. There is much interest in the miniaturization of devices for these measurements. A frequently studied device is the chemically sensitive field-effect transistor (CHEMFET), in which the gate region of a field-effect transistor is made sensitive to chemical events through their effect on the gate potential. The CHEMFET was first described in 1970 (1) and has been the subject of several reviews (2-4). Here we describe a simple alternative semiconductive structure, the light-addressable potentiometric sensor (LAPS). Brief descriptions of some aspects of this work have been presented elsewhere (5-7).

Both LAPS and CHEMFET are insulated semiconductor devices that respond to surface potentials at an electrolyte-solid interface through the effect of such potentials on electric fields within the semiconductor. Surface potentials can be established by chemically selective surfaces that acquire electrical charge in response to changes in chemical properties of an electrolyte. In addition, the electric fields within the semiconductor can be modulated by transmembrane potentials when the membranes are appropriately positioned relative to the insulated semiconductor surface. Attractive features of the LAPS include potentiometric stability and the ability to address different

regions of the semiconductor with light rather than with fixed wires or other current paths. As discussed below, potentiometric stability implies sensitivity in biochemical determinations such as enzyme-linked immunoassays. The ability to optically address different spatial regions of a sensor surface allows multiple potentiometric measurements to be made with a single semiconductor device.

Figure 1a shows the insulated surface of a thin flat plate of *n*- or *p*-type silicon in contact with an electrolyte. The insulator separating the electrolyte from silicon is a layer of silicon oxynitride approximately 1000 Å thick. The direct current through this insulating layer is negligible, less than a picoampere per square centimeter under the experimental conditions described below. In Fig. 1a, a potential  $\Psi$  is shown applied from the silicon plate to a Ag/AgCl controlling electrode. This controlling electrode also serves as a reference electrode in that it fixes the potential from the variable potential source to solution. The sign and magnitude of  $\Psi$  can be adjusted so as to deplete the semiconductor of majority charge carriers at the insulator interface. In this state the semiconductor produces a transient photocurrent in response to transient illumination either from above or below the silicon plate. An intensity-modulated light source, such as one of the light-emitting diodes (LEDs) A through D in Fig. 1a, gives rise to an alternating photocurrent through the indicated circuit. The amplitude of the alternating current (*I*) is measured with a low-impedance ac ammeter. Many configurations of semiconductor, light source, controlling electrode, and reference electrode (if needed) are possible (Fig. 1b). The value of *I* depends on the applied bias potential  $\Psi$  (Fig. 2). This photocurrent varies from a minimum value of near 0 under forward bias conditions to a maximum value limited by

the minimum attainable depletion layer capacitance under reverse bias conditions (8). Electrical circuits can be devised that sweep the bias potential with time while simultaneously multiplexing a series of LEDs that illuminate different sites on the silicon surface. We have measured the surface potential at nine different sites once every second using this approach. This time includes the time required to compute the potential  $\Psi_i$ , which is the potential where the slope ( $dI/d\Psi$ ) is maximum, and present the values of the  $\Psi_i$  on a personal computer. In Fig. 1a different surface structures or chemistries, or both, at different positions are indicated schematically. Such structures include those that are sensitive to *pH*, redox potential, or transmembrane potential.

Previous work has shown that silicon oxynitride is *pH*-sensitive over a large *pH* range. Such measurements have been performed with the oxynitride on the gate region of an FET (9) or alternatively by monitoring the voltage dependence of the capacitance of the semiconductor-insulator interface (10-12). This *pH* sensitivity is due

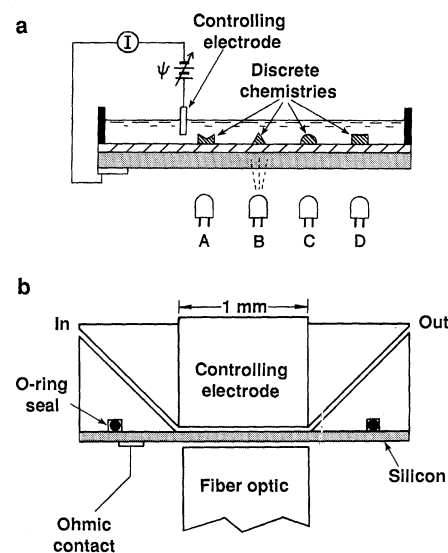


**Fig. 1.** Light-addressable semiconductor sensors. (a) A silicon plate with a surface insulator of oxynitride (diagonal lines) in contact with an electrolyte is photoresponsive to the light emitting diodes A, B, C, and D. The resultant alternating photocurrent *I* in the external circuit depends on the applied bias potential  $\Psi$ . Different chemistries located on different regions of the insulating surface produce variations in the local surface potential that can be determined by selective illumination with one or another of the light-emitting diodes. (b) For high-sensitivity measurements of enzyme activity it is advantageous to localize the enzyme molecules in a small volume so that they are present at a high effective concentration. Volumes as small as a nanoliter can be achieved with a configuration such as the one illustrated. The controlling electrode acts as a piston. It can be raised to allow fluid to be passed over the sensor surface and then lowered to create the small reaction volume.

Molecular Devices Corporation, 3180 Porter Drive, Palo Alto, CA 94304.

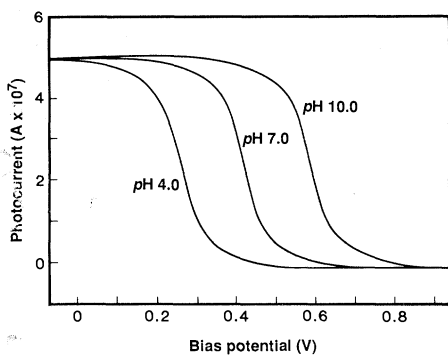


**Fig. 2.** Alternating photocurrent ( $I$ ) as a function of bias potential ( $\Psi$ ) for different values of  $pH$ . The photocurrent for a circuit such as that illustrated in Fig. 1 depends on the bias potential. Positive values of  $\Psi$  indicate that the controlling electrode is biased positively with respect to the silicon. The data illustrated are for  $n$ -type silicon, where the lower voltages (to the left) correspond to the depletion condition for the semiconductor at the insulator interface. For  $p$ -type silicon the shape of the curve is reversed, left to right. The surface in contact with the electrolyte is silicon oxynitride, which is  $pH$  sensitive.

to the proton binding capacity of Si-O and Si-NH<sub>2</sub> groups on the silicon oxynitride surface (13). Figure 3 shows that the  $pH$  response over a range from 2 to 12 of the LAPS device at an oxynitride site is Nernstian.

Redox potential measurements can be made by depositing pads of metallic gold 5000 Å thick over the insulating silicon oxynitride coating on silicon plates. When the electrolyte solution contains a redox pair such as ferricyanide-ferrocyanide, the potential of the gold is determined by the ratio of the concentrations of these two species, in accordance with the Nernst equation. Thus intensity-modulated illumination of a region of the semiconductor beneath the gold pad produces an alternating photocurrent similar to that observed with the  $pH$  sensing device. In this case, however,  $\Psi_i$  responds to changes in redox potential of the electrolyte.

When a membrane is interposed between the controlling-reference electrode and the silicon, a transmembrane potential will add in series with  $\Psi$  and thus affect the photoresponse. Transmembrane potentials are also often Nernstian and can be conveniently considered along with  $pH$  and redox. Figure 3 shows a Nernstian potential response arising from potassium ions when a valinomycin-containing membrane on top of an oxynitride-coated silicon plate is placed in contact with solutions containing various concentrations of potassium chloride.

Figure 4 illustrates the response that is observed when two chemically distinct regions are illuminated simultaneously with a single intensity-modulated light source. One region is a silicon oxynitride surface and the

other is a gold pad deposited on top of oxynitride. The intensity-modulated light beam is expanded in diameter so that the illuminated area is approximately twice as large as the gold spot. Upon sweeping the value of  $\Psi$ , two inflections in the  $I$  versus  $\Psi$  curve are seen. The potential at the inflection point seen near  $-0.1$  V is responsive to  $pH$ . The potential at the inflection point seen near  $-0.9$  V is responsive to redox potential. When the solution contains a redox buffer, such as a mixture of ferri- and ferrocyanide, the potential from the gold to solution is fixed, and changes in the photoresponse from the oxynitride region can be used to measure changes in the  $pH$  of the solution. The signal from under the gold-covered area acts as a reference. When the solution is buffered with respect to  $pH$  and a redox chemical reaction takes place, the potential from the gold to solution will change. This change in solution redox potential can be measured by using the signal from the oxynitride region as a reference. This internal reference mechanism allows for  $pH$  and redox measurements to be carried out simultaneously at different illuminated sites. In this case the controlling electrode can be simplified (for example, a piece of wire in contact with solution) since it need not act as a reference.

An area of application of the LAPS device is in the high-sensitivity measurements of enzyme activity as used, for example, in enzyme-linked immunoassays. Appropriate enzymes are those that produce  $pH$  changes or changes in redox potential. For simplicity we equate sensitivity with the number of enzymes that can be detected with quantitative accuracy, as this is often the criterion of practical interest. Two features of the LAPS device contribute to high sensitivity. First, the device has high potentiometric stability. A drift in surface potential of less than 0.1  $\mu$ V per second can be achieved, which corresponds to 1.7 micro  $pH$  units per second. Second, when the enzymes to be detected are trapped or immobilized near the semiconductor surface, the buffering effect of the electrolyte can be minimized by reducing the volume of the solution in contact with the insulated semiconductor surface. Figure 1b illustrates a cell designed to provide a small fluid volume in contact with the insulator surface. The sensitivity of a small volume system of this sort to detect an enzyme that produces a  $pH$  change following substrate turnover can be calculated as follows. Let the enzyme turnover number to produce or consume protons be  $n$  (with units of moles of protons per second per mole of enzyme), and let  $v$  be the number of moles of  $pH$  change of solution is

$$d(pH)/dt = en/(Bv + bs) \quad (1)$$

where  $B$  is the volumetric buffer capacity of the electrolyte,  $v$  is the volume of the solution,  $b$  is surface buffer capacity of the chamber surfaces, and  $s$  is the surface area of the chamber in contact with the electrolyte. The volumetric buffer capacity of the solution is

$$B = 2.303 [a - (a^2/c)] \quad (2)$$

where  $c$  is the molar concentration of the buffer and  $a$  is the molar concentration of the acidic species of the buffer pair. An equivalent expression for  $b$  is obtained in which the concentrations of buffer species are given in terms of surface concentration or in units of moles per square centimeter. According to Eq. 1, the sensitivity to detect a given number of enzymes from a  $pH$  change can be increased by decreasing the volume or volumetric buffer capacity. Decreasing the volumetric buffer capacity by reducing the buffer concentration below 1 mM or adjusting the initial solution  $pH$  to be far from the buffer  $pK$  is generally not practical, as substantial  $pH$  drifts will occur due to equilibration of atmospheric CO<sub>2</sub> with solution. For a fixed buffer concentration in the electrolyte, the rate of  $pH$  change can be increased by reducing the electrolyte volume  $v$  until the surface buffer capacity of the chamber becomes dominant, as indicated in Eq. 1. The data given in Fig. 5 illustrate the determination of surface buffer capacity of a sample cell. In this experiment, the sample volume is estimated to be of the order of 1 nl, and the surface buffer is about

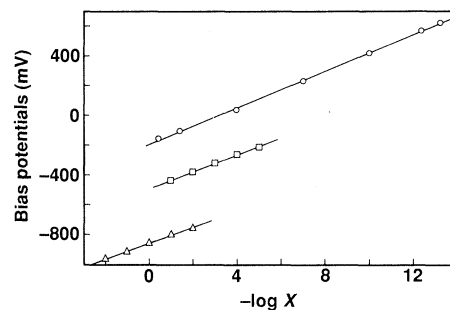


**Fig. 3.** Nernstian responses to electrolyte composition. This graph shows plots of potential ( $\Psi_i$ ) at maximum photocurrent slope (maximum  $dI/d\Psi$ ) for three different chemically sensitive surfaces on the semiconductor. For  $X = [H^+]$ , the proton concentration (data points are given by circles) shows that the photoresponse is Nernstian over a  $pH$  range greater than from  $pH$  2 to 12. The sensing surface is silicon oxynitride. For  $X = [ferricyanide/ferrocyanide]$ , the data points are given by triangles, and the surface is gold over silicon oxynitride. For  $X = [K^+]$ , data points are given by squares, and the sensing surface is a membrane over the oxynitride. The membrane is 66% polyvinylchloride, 33% dioctyladipate, and 1% valinomycin [see (14)].

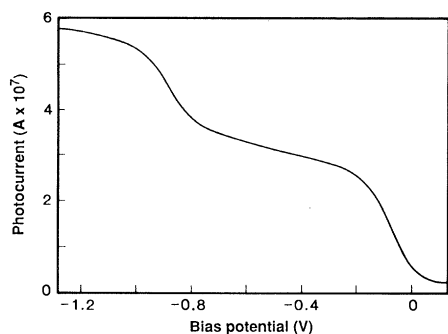


**Fig. 4.** Biphasic response for a binary sensing surface. In this experiment, a single light-emitting diode illuminates an area under a surface that is approximately 50% silicon oxynitride in contact with the electrolyte and 50% gold on silicon oxynitride in contact with the electrolyte. The solution is buffered at  $pH$  7.4 and contains 5  $mM$  ferricyanide and 5  $mM$  ferrocyanide. The biphasic response originates from the different surface potentials for the two cases. The inflection on the left is associated with the gold surface (redox potential) and that on the right is associated with the silicon oxynitride surface ( $pH$ ).

1 pmol, which limits the sensitivity according to Eq. 1; about 10,000 molecules of an active enzyme such as urease,  $n = 5,870$  (15), should give a rate of  $pH$  change significantly above the background drift stated above.

Enzyme-linked redox chemistry can be used for a number of biochemical and immunochemical assays (16–18). The theoretical sensitivity for a redox measurement is limited by the metal-electrolyte interfacial capacitance, which is of the order of 20  $\mu F cm^{-2}$ . This capacitance must be charged by exchange of electrons to or from the redox species. The requirement for charging this interfacial capacitance in order to generate a change in surface potential determines the ultimate theoretical sensitivity of this sensor for the measurement of changes in both redox potential and  $pH$ .

The experiments described in this report have all been performed with an illumination area of about 1  $mm^2$ . For the silicon used, the minority-carrier diffusion length is on the order of 1  $mm$ , which means that the measured photocurrent is obtained from an area of approximately 1  $mm^2$  even if the surface chemistry of interest is confined to a smaller area. High spatial resolution can in principle be achieved in several ways. The silicon can be masked, for example, with a thick insulating layer, so as to allow only a very small area of the silicon oxynitride surface to come in contact with the aqueous medium. Silicon can be doped with gold to reduce the minority carrier lifetime and thus reduce diffusion lengths. The frequency of modulation of the illumination source can be increased. Phase-sensitive detection of the photocurrent will also in-

crease spatial resolution.

For the purpose of discussing signal-to-noise ratio in the LAPS device, the signal is defined as the slope of the midpoint region of the photocurrent versus potential curve (Fig. 2), and noise is the time-dependent variation of photocurrent amplitude at that potential. The signal, or slope of the photocurrent curve, is a function of the absolute amplitude of the photocurrent and the width of the curve given by the first derivative of photocurrent versus potential. Typical full-widths at half-height for first derivative photoresponse curves are approximately 0.1 V at low photocurrents. The photocurrent increases linearly with increasing illumination intensity up to the point where the alternating photopotential generated across the insulator approaches the width of the photoresponse curve. At this point, a further increase in illumination intensity results in an increase in width of the photoresponse curve and thus tends to negate the increase in signal due to an increase in photocurrent. Therefore the optimum photocurrent  $I$  is approximated by the equation

$$I \sim EC/t \quad (3)$$

where  $E$  is the width of the photoresponse curve (0.1 V),  $C$  is the capacitance of the oxynitride insulator ( $0.05 \mu F cm^{-2}$ ), and  $t$  is the illumination time per modulation cycle (0.05 msec for 10-kHz square-wave modulation). This optimum photocurrent is  $\sim 1 \mu A mm^{-2}$ . In general, to optimize signal-to-noise ratio the input impedance of the photocurrent amplifier is matched to the sensor impedance. In the case of the LAPS, however, this strategy results in cross talk between various chemistry sites. To minimize this cross talk, most of the photocurrent must flow into the input amplifier. This is accomplished by making the input impedance of the amplifier small with respect to the sensor impedance. In this configuration, the major source of noise is the equivalent input voltage noise of the first operational amplifier (current to voltage converter). Because the sensor acts as a shunting capacitor from this input to ground, the noise is essentially proportional to frequency in the frequency range of interest (about 10 kHz). Varying the illumination modulation frequency in this range does not alter significantly the signal-to-noise ratio, as the signal also is proportional to frequency (Eq. 3).

Two features, the planar surface of the device and the ease with which multiplicity can be achieved by addressing discrete sensing sites with light, make the device described in this report an ideal candidate for use as a signal transducer in biosensors. In biosensors, the most difficult component to control is the biological or biochemical com-

ponent. Enzymatic reactions are temperature-sensitive, proteins tend to denature and become inactive as a function of time and their environmental history, and even at the level of manufacturing, different preparations of the same biological material often result in different levels of biological activity. For these reasons a robust biosensor should have a variety of “on-board” biochemical calibrators. The light-addressable aspect of the LAPS makes sensing a multiplicity of on-board calibrators a relatively straightforward task. To date we have measured the kinetics of reactions run simultaneously at as many as 23 sites on a single sensor with only two electrical leads from the controlling

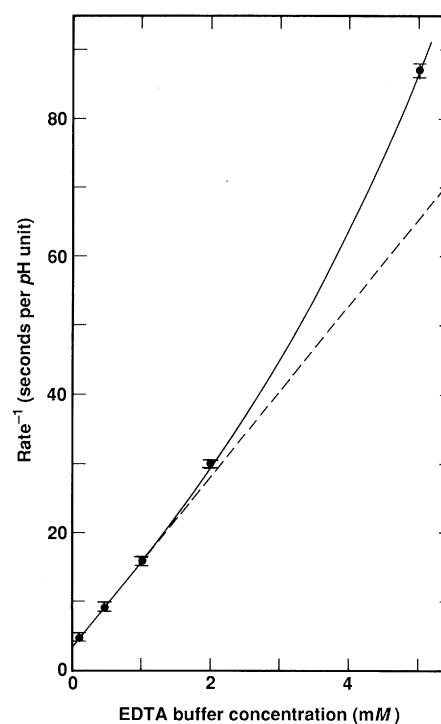


**Fig. 5.** Determination of sensor-surface buffer capacity. The rate of  $pH$  change as a function of substrate buffer concentration was determined using urease as the  $pH$  changing enzyme. Urease was nonspecifically adsorbed to the surface of the silicon. The solution contained 16  $mM$  urea, 150  $mM$  NaCl, and various concentrations of EDTA ( $pH$  5.7) as indicated. The sensing chamber was a cylinder with a diameter of 3  $mm$  and a height of approximately 0.2  $\mu m$ . The height of the chamber could be temporarily increased to allow for introduction of fresh substrate and buffer. Two separate measurements were performed at each buffer concentration, except for 0.1  $mM$  EDTA, where four measurements were taken. The data are corrected for an apparent first-order loss of urease activity with successive buffer replacements in the flow cell. The error bars indicate the range of the data points. The solid line connects the data points. The dashed line is a linear fit to the first three data points. Deviation of the points from the linear fit at 2  $mM$  and more strongly at 5  $mM$  EDTA is probably due to inhibition of urease due to accumulation of ammonia. For urease the inhibition constant for ammonia is 10  $mM$  (19).

electronics to the sensor. Furthermore, by partially covering the surface with metal, separate pH and redox measurements can be made at each site to control for potentiometric stability of the system if one or the other of these solution parameters is made stable at each site by an appropriate buffer. Another feature of the LAPS that lends convenience to the fabrication of biosensors is its planar surface. The flat polished sensing surface has two significant attributes. First, it is easy to create fluid seals to maintain the aqueous solution only in contact with the insulator surface. For high-sensitivity assays, microscopic fluid leaks between the aqueous compartment and the electrical contact on the back side of the semiconductor can result in substantial potentiometric drifts. For some sensor configurations, a resistive path of 100 gigaohms through the fluid leak into a small volume can result in substantial drifts. Second, the flat surface makes it possible to generate very small, defined aqueous volumes. These volumes can be as small as a nanoliter. The advantage of using small volumes for performing high-sensitivity assays is discussed above. We have detected one attomole (600,000) of enzyme molecules adsorbed to filter paper 100  $\mu\text{m}$  thick. The time required to make this determination was approximately 2 minutes.

The principal advantage of biosensors, such as the one described here, is the ease with which miniaturization can be achieved. This miniaturization in turn facilitates multiplicity and high sensitivity. Specific applications of this methodology to enzyme-linked immunochemical assays for therapeutic drugs, hormones, and bacterial pathogens will be given elsewhere.

#### REFERENCES AND NOTES

- P. Bergveld, *IEEE Trans. Biomed. Eng.* **BME-19**, 70 (1970).
- J. Janata and R. J. Huber, in *Ion-Selective Electrodes in Analytical Chemistry*, H. Freiser, Ed. (Plenum, New York, 1980), pp. 107-174.
- J. N. Zemel, *Anal. Chem.* **47**, 255A (1975).
- G. F. Blackburn, in *Biosensors Fundamentals and Applications*, A. P. F. Turner, I. Karube, G. S. Wilson, Eds. (Oxford Univ. Press, Oxford, 1987), pp. 481-530.
- H. M. McConnell, J. W. Parce, D. G. Hafeman, *Electr. Soc. Abstr.* **87**, 2272 (1987).
- \_\_\_\_\_, *Proc. Electrochem. Soc.* **87**, 292 (1987).
- D. G. Hafeman, J. W. Parce, H. M. McConnell, *Proceedings of the 2nd International Meeting on Chemical Sensors*, J. L. Aucouturier et al., Eds. (Bordeaux, 1986), p. 69.
- For a general reference on semiconductor photoresponses, see S. N. Sze, *Physics of Semiconductor Devices* (Wiley, New York, 1981), pp. 362-430.
- L. Bousse, P. de Rooij, P. Bergveld, *IEEE Trans. Electr. Dev.* **ED-30**, 1263 (1983).
- Y. G. Vlasov, A. J. Bratov, V. P. Letavin, in *Ion-Selective Electrodes 3*, vol. 8 of the *Analytical Chemistry Symposium Series*, E. Pungor, Ed. (Elsevier, Amsterdam, 1981), pp. 387-397.
- F. Chauvet, A. Amari, A. Martinez, *Sensors Actuators* **6**, 255 (1984).
- M. T. Pham and W. Hoffmann, *ibid.* **5**, 217 (1984).
- L. Bousse and J. D. Meindl, *ACS Symp. Ser.* **323**, 79 (1986).
- U. Oesch, D. Ammann, W. Simon, *Clin. Chem.* **32**, 1448 (1986).
- R. L. Blakeley and B. J. Zerner, *J. Mol. Catal.* **23**, 263 (1984).
- W. U. de Alwis, B. S. Hill, B. I. Meiklejohn, G. S. Wilson, *Anal. Chem.* **59**, 2688 (1987).
- D. S. Wright, H. B. Halsall, W. R. Heineman, *ibid.* **58**, 2995 (1986).
- F. A. Armstrong, H. A. O. Hill, N. J. Walton, *Q. Rev. Biophys.* **18**, 261 (1986).
- L. Goldstein, M. Levy, L. Shemer, *Biotechnol. Bioeng.* **25**, 1485 (1963).
- We are greatly indebted to G. Pontis, J. Kercso, and L. Bousse for helpful discussions and technical assistance. Supported in part by the Army Research Office and Defense Advanced Research Projects Agency.

8 February 1988; accepted 20 April 1988

## Crystal Structure of Hexaazaoctadecahydrocoronene Dication $[\text{HAOC}]^{2+}$ , a Singlet Benzene Dication

JOEL S. MILLER, DAVID A. DIXON, JOSEPH C. CALABRESE

The structures of hexaazaoctadecahydrocoronene,  $[\text{HAOC}]^n$  ( $n = 0, +2$ ), have been determined by single-crystal x-ray diffraction. Although HAOC is aromatic, its dication has a localized structure that is based upon Jahn-Teller-distorted cyanine/*p*-phenylenediammonium fragments. The structure is consistent with the singlet ground state as determined by magnetic susceptibility and contrasts with the simplest Hückel expectation of a triplet ground state.

THE MCCONNELL CONJECTURE (1, 2) has focused research toward the design and synthesis of stable organic molecules with triplet ground states in order to prepare a molecular/organic ferromagnet (3-6). Recently this goal has been achieved with the characterization of  $[\text{Fe}^{\text{III}}(\text{C}_5\text{Me}_5)_2]^+[\text{TCNE}]^-$  (TCNE = tetracyanoethylene) as a bulk ferromagnet (3, 7). This mechanism requires stable radicals with a degenerate highest occupied molecular orbital (HOMO) that is not half-filled. Thus the radicals must possess a rotation axis of order  $n \geq 3$  or have  $D_{2d}$  symmetry (2, 3, 8). Organic radicals such as the radical cations of HAOC (Fig. 1) or hexaamino-benzene (9) are examples of such materials. HAOC has been prepared (10, 11) and its dication,  $[\text{HAOC}]^{2+}$ , has been reported to have a ground-state triplet (6, 10, 12). Based upon these observations, we have prepared several salts of  $[\text{HAOC}]^{2+}$  with donor-acceptor radical anions of the type that have been previously reported to stabilize ferromagnetic coupling as the  $[\text{Fe}^{\text{III}}(\text{C}_5\text{Me}_5)_2]^+$  salt and observe only diamagnetic behavior (13). These results are surprising, as a simple Hückel model of the benzene  $\pi$ -system leads to the prediction of a triplet for the dication as previously reported for  $[\text{C}_6\text{Cl}_6]^{2+}$  (14). Since we sought to understand the diamagnetic behavior and since these high-symmetry, low-ionization potential donors are of theoretical interest, we prepared  $[\text{HAOC}]^n$  ( $n = 0, 1+, 2+$ ) as crystalline solids, and we

report the structure and magnetic properties of  $[\text{HAOC}]^n$  ( $n = 0, 2+$ ).

We prepared HAOC from hexaamino-benzene via a modified literature route (5, 10, 11, 13) and studied its single-crystal x-ray diffraction (15). The colorless crystals possess inversion crystallographic symmetry, and the idealized molecule belongs to the  $D_{3d}$  point group. The  $[\text{HAOC}]^{2+}$  cation was prepared by oxidation with  $\text{Ag}^+$ , and the 1:2 salts with  $[\text{BPh}_4]$  (Ph, phenyl),  $[\text{BF}_4]^-$ , and  $[\text{PF}_6]^-$  have been isolated as stable crystalline solids. The red crystals of  $[\text{HAOC}]^{2+}$  as either the  $[\text{BF}_4]^-$  (16) or  $[\text{PF}_6]^-$  (17) salts have inversion crystallographic symmetry, and the idealized dication belongs to the  $C_{2h}$  point group. The dications are isolated from each other, as there are no intermolecular interactions less than 3.5 Å and the stacking is such that the benzene rings do not directly overlap. The average bond distances for HAOC and  $[\text{HAOC}]^{2+}$  are listed in Table 1.

Cyclic voltammetry of HAOC showed that it has four reversible one-electron oxidations at -0.44, +0.06, +0.52, and +0.92 V ( $\pm 0.01$  V) versus a standard calomel electrode (MeCN solvent) for the 0/1+, 1+/2+, 2+/3+, and 3+/4+ redox couples, respectively (13). The differences between potentials are comparable to previously reported values, although the absolute values deviate with those previously reported by +0.33  $\pm$  0.03 V (10).

The structures of HAOC and  $[\text{HAOC}]^{2+}$  have the common feature of an approximately planar  $\text{C}_6\text{N}_6$  moiety. The structure of HAOC has an aromatic benzene ring. Upon oxidation to the dication, the a and b C-C

Central Research and Development Department, Experimental Station E328, E. I. du Pont de Nemours & Company, Inc., Wilmington, DE 19898.